PHYSICAL REVIEW B VOLUME 23, NUMBER 6 15 MARCH 1981

Theory of defect states in glassy As_2Se_3

David Vanderbilt and J. D. Joannopoulos
Department of Physics, Massachusetts Institute of Technology, Cambridge, Massachusetts 02139
and Center for Materials Science and Engineering, Massachusetts Institute of Technology, Cambridge, Massachusetts 02139
(Received 30 July 1980)

Structural defects in glassy As_2Se_3 are classified and labeled according to the constituent like-atom bonds and malcoordinated atoms. A selection rule is formulated to reduce the number of allowed Fermi-level pinning reactions. An elementary Bethe-lattice model is introduced as a starting point for a discussion of the electronic structure of simple defects. The defect states are found to be very different from those in Se; deep gap states arise in As_2Se_3 because of unique bond orbitals, whereas they occur in Se due to unique π interactions between orbitals. Malcoordinated Se atoms are expected to give rise to *hydrogenic* levels in As_2Se_3, in contrast to Se. Surprisingly, the undercoordinated pnictide defects are *positively* charged in this model. Finally, defect creation energies and densities at T_g are discussed.

I. INTRODUCTION

In recent years, there has been considerable progress made in both experimental and theoretical aspects of the study of chalcogenide glasses. Much of this work was stimulated by Anderson's hypothesis that a strong electron-phonon coupling could give rise to a spin-pairing "negative U," thereby explaining the pinning of the Fermi level in the absence of paramagnetism.[1] Several more detailed models have since been proposed. Some[2,3] assumed that the one-electron gap is washed out by a smooth distribution of bond strengths, and invoked two-electron effects to explain the experimental properties of the glasses. On the other hand, the defect models put forward by Mott, Davis, and Street[4] and Kastner, Adler, and Fritzsche[5] assigned the negative U and other experimental properties to distinct structural defects in the glass. This approach is based on the idea that the distribution of bond strengths remains sharply peaked (i.e., that weak bonds are *less* likely to occur than broken or extraordinary bonds) because covalently bonded atoms tend to seek one of a few natural bonding configurations. The interconversion of these coordination defects, with their associated gap states, is then used to explain the negative U, the Stokes-shifted photoluminescence, the photoinduced ESR and IR absorption, and other experiments.[4-6] Finally, it should be pointed out that several other defect-related models have been suggested,[7-10] including the recent raft model of Phillips.[7] Also, Emin has proposed a model based on small polarons.[11]

Quite recently, the defect model has received new support from experiments which shed light upon the photoluminescence mechanism,[12] the valence alternation pair (VAP) radial distribution function,[12,13] and the density of states in the gap.[13-15] However, these experiments are generally *not* sensitive to the bonding configuration of the defects involved, so that identification of defects remains highly model dependent. It is here that theory can play a role. For example, recent work,[16,17] based upon total energy calculations and identification of gap states responsible for the photoinduced ESR, has led to the surprising result that the neutral defect in glassy Se is onefold, rather than threefold, coordinated.

Unfortunately, however, theory and experiment have not yet combined to give a coherent picture of the defects responsible for the properties of chalcogenide glasses. In large measure, this is due to the fact that experiments are usually more conveniently done on As–Se and As–S glasses, whereas the theory tends to focus on the simpler case of glassy Se. Experimentally, some of the properties of heteropolar and homopolar glasses appear similar, and the distinction between the two is often blurred. However, there are important differences. For example, both the photoluminescence efficiency and photoinduced ESR intensity are much lower in Se than in As_2Se_3, and both experiments show quite different dopant dependencies in the two cases.[18] Moreover, it is now becoming clear that the properties of individual defects in As_2Se_3 and Se are expected to be quite different. The coordination defects in glassy Se have deep gap states whose origin can be traced to an anomalous π-bonding mechanism which does *not* carry over to the case of heteropolar glasses.[19] Thus the corresponding deep gap states are *not* expected in As_2Se_3. On the other hand, the heteropolar glass allows for anomalous bond orbitals (like-atom bonds and nonbonding As orbitals) which will give rise to deep gap states having no counterpart in pure Se.[20] Clearly the two kinds of systems must be treated quite differently.

In this paper, we will attempt to bridge some of these gaps by applying the ideas developed in the

study of glassy Se (Ref. 18) to the case of As_2Se_3. Because the structures are more complicated and the defect possibilities more numerous in As_2Se_3, serious theoretical calculations are still in their infancy. Nevertheless, by using some simple models, and arguing by analogy with the case of Se where appropriate, we will be able to say quite a bit about the nature of intrinsic structural defects in the heteropolar glass. The discussion will be carried out using As_2Se_3 as a model system, but many of the conclusions may be applicable to sulfide or telluride glasses as well.

In Sec. II, we discuss various methods for classifying defects, and attempt to identify those defects which are most likely to occur. Section III provides a detailed discussion of the electronic structure of the various defects, with an emphasis on similarities and differences with respect to Se. In Sec. IV we present a speculative discussion of defect total energies, and discuss the structural equilibrium at T_g which determines the defect densities in the glass. Finally, we summarize our results in Sec. V.

II. CLASSIFICATION OF DEFECTS

In order to introduce the concept of defects, we must first define what is meant by a glass that has no defects. To visualize such a "perfect glass," consider a continuous random network such as the one shown in Fig. 1(a). Every As atom has its preferred threefold coordination satisfied, every Se atom has its preferred twofold coordination satisfied, and every bond is heteropolar. We will adopt the point of view that the perfect glass is the lowest-energy disordered structure, and that every deviation from the perfect-glass structure costs energy.

Such deviations take the form of various point defects in the glass. Figure 1(b) shows an amorphous network in which As and Se atoms retain their preferred coordination, although a large number of "wrong[9]" or like-atom bonds (LAB's) occur. On the other hand, Fig. 1(c) depicts a structure containing many malcoordinated[21] atoms (MCA's), but no LAB's. If the system tries to lower its energy by minimizing the number of LAB's and MCA's present,[22] then we expect the material to consist of a "bulk" network having the perfect-glass structure, interrupted occasionally by a defect containing one or more LAB's or MCA's.

A sampling of possible defect configurations is given in Fig. 2. The defects have been categorized according to the number of MCA's and LAB's they contain. Thus, our energy minimization principle implies that the defects in the upper left-hand region of the chart are the most likely ones, other things being equal. We have developed a notation which uniquely designates each defect; these are shown to the right of each configuration. The letters C and P correspond to chalcogen and pnictide,

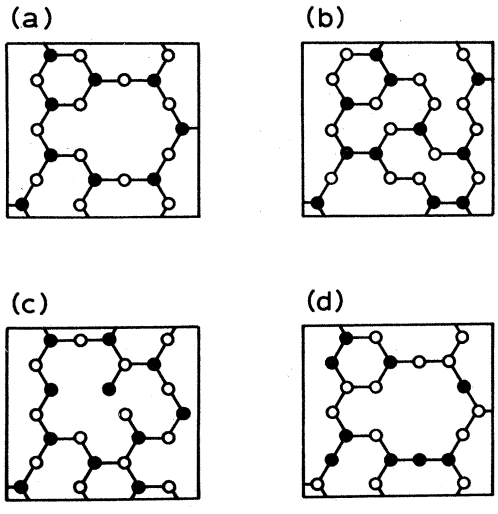

FIG. 1. Schematic diagram of a random network with (a) no defects, (b) many like-atom bonds but no coordination defects, (c) many malcoordinated atoms but no like-atom bonds, (d) many malcoordinated atoms but no like-coordinated-atom bonds. Solid circles represent As, open circles Se.

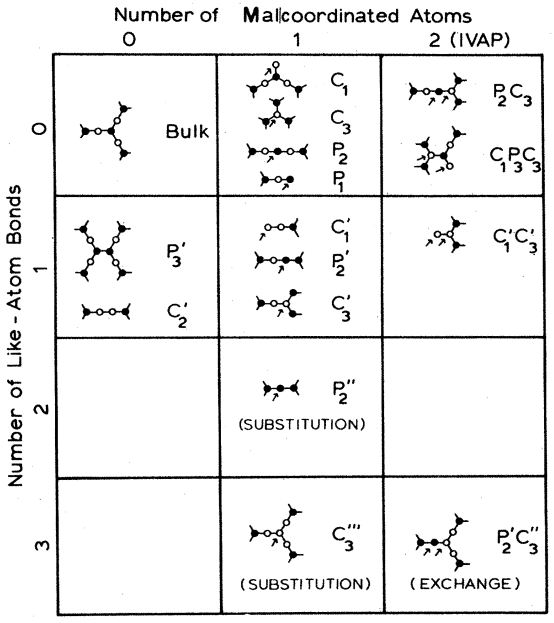

FIG. 2. Defect topologies organized according to number of malcoordinated atoms (marked by arrows) and number of like-atom bonds. Solid circles As, open circles Se. External bonds are understood to connect to a chalcogen atom of the bulk glass structure.

respectively, and the subscript denotes the coordination, following many previous authors. Each superscript prime indicates one LAB connected to that site, and multiple MCA's are represented using a molecular notation for the smallest cluster of sites which includes all the MCA's.

Obviously there are many more possibilities for defects than are shown in Fig. 2; we have attempted to include the simplest and most interesting ones. The most elementary defects are the single MCA's (C_1, C_3, P_2, P_1) and the single LAB's (P_3', C_2'). (P_4 has been left out because the s-p hybridization puts it in a class by itself.) The simplest close defect pairs ("intimate valence alternation pairs" or IVAP's)[5] are the nearest-neighbor pairs P_2C_3 and $C_1'C_3'$ and the second-neighbor pair $C_1P_3C_3$. If a Se is substituted for an As (or vice versa) a C_3''' (or P_2'') center results; an interchange of neighboring Se and As atoms gives rise to a $P_2'C_3''$ IVAP. Phillips's outrigger contains a C_2''.[7]

Note that the substitutions and interchanges have the property of conserving the structure of the bulk glass, as can be seen by comparing Figs. 1(a) and (d). In particular, they allow the system to avoid bonds between like-coordinated atoms. (That is, twofold coordinated sites are always bonded to threefold sites, and vice versa.) We shall use the term "like-coordinated-atom bond" (LCAB) for a bond connecting two sites with the same coordination number, in analogy to like-atom bonds (LAB's). If it is energetically favorable for the glass to avoid LCAB's, we say the LCAB principle is in force. This possibility provides an alternative to the LAB principle, assumed earlier, which supposes that like-atom bonds are unfavorable. In the absence of MCA's, a LCAB is a LAB and vice versa, but different coordination defects will be expected depending on which principle is in force.

The LAB principle can be given a physical motivation, based on the fact that the partial ionic character of a heteropolar bond makes it stronger than the average of the two different homopolar bonds. The difference ΔE in bond energies D can be estimated from the As–Se electronegativity difference $\Delta\chi$ (Ref. 9):

$$\Delta E \equiv D(\mathrm{As}-\mathrm{Se}) - \tfrac{1}{2}[D(\mathrm{As}-\mathrm{As}) + D(\mathrm{Se}-\mathrm{Se})] \cong (\Delta\chi)^2 = 0.2 \quad (1)$$

expressed in units of eV. Thus the fraction of like-atom bonds frozen in at the glass transition temperature is expected to be on the order of $\exp(-\Delta E/kT_g) \cong 5\times10^{-3}$. Put another way, this argues that a defect with n LAB's is at least 100 times as likely as a similar defect with $n+1$ LAB's. However, the foregoing assumes that the energy cost of a LAB is independent of its local environment. It probably is not; for example, one could argue that a C_3 atom will be more electropositive than a normal C_2, and may therefore allow chalcogen neighbors at no extra cost in energy. Moreover, an argument can be made in favor of the LCAB principle if one assumes that the continuous random network consists of a disordered arrangement of layers with the internal structure of those in the crystal. In that case, defects which preserve the layer structure will be favored. The LCAB-free defects (basically As–Se substitutions) are of this structure-preserving type.

The same argument applies much more certainly to structural defects in crystalline As_2Se_3. Alternative defects (e.g., vacancies, or interstitials covalently bonded to neighboring layers) introduce a minimum of two MCA's, while a simple substitution has only one MCA and is entirely strain free. In fact, the assumption that the LCAB principle dominates the crystal while the LAB principle dominates the glass may provide a natural explanation for the higher photoluminescence quantum efficiency and absence of fatigue in crystalline As_2Se_3 (Ref. 23) if the dominant nonradiative center in the glass contains a LCAB. For definiteness, we will proceed on the assumption that the LAB principle dominates in the glass, but we will pay special attention to the substitution and interchange defects as we go along.

Table I shows an alternative classification scheme which is also instructive. Defects have been categorized according to two properties: (i) The "natural charge state" (the charge on the defect when all the valencelike states are filled with electrons and all the conductionlike states empty; that is, when no carriers are trapped), and (ii) the "chalcogen excess." The latter is defined as the number of Se atoms, over and above the usual As_2Se_3 ratio, introduced by the defect. For ex-

TABLE I. Classification of defects according to chalcogen excess and natural charge state.

Chalcogen excess	Natural charge state +2	+1	0	−1
$\frac{3}{2}$				C_1'
1			C_2', $C_1'C_3'$	
$\frac{1}{2}$		P_4, C_3' ⟷		C_1
0	$P_2'C_3''$ ⟷		$C_1P_3C_3$	
$-\frac{1}{2}$		C_3, P_2		
−1	P_1, P_2C_3 ⟷		P_3'	
$-\frac{3}{2}$		P_2'		

ample, if an As–Se bond in the bulk is broken and an extra Se atom inserted, a C_2' (Se LAB) defect results; thus the chalcogen excess of this defect is $Q_c(C_2') = +1$. Similarly, a Se atom removed from the bulk creates *two* P_2 defects, so that $Q_c(P_2) = -\frac{1}{2}$. The chalcogen excess of any defect can be obtained in this way. The glass can thus become Se rich (As rich) by incorporating defects with $Q_c > 0$ ($Q_c < 0$).

This stoichiometry dependence is not the only interesting feature of the chalcogen excess. The defect model has been able to explain Fermi-level pinning in the absence of paramagnetism by the interconversion of defects from one natural charge state to another.[4,5] For example, the reaction $(C_1)^- \rightharpoonup (C_3')^+$ is accomplished by breaking (reforming) a bond. However, the reaction $C_1^- \rightharpoonup C_3^+$ is impossible because breaking a bond adjoining the C_3 results in a P_2, not a C_1. We can systematize these considerations by noting that $Q_c(C_1) = +\frac{1}{2}$ while $Q_c(C_3) = -\frac{1}{2}$, so that the reaction $C_1 \rightharpoonup C_3$ can only occur if a Se atom is physically removed from the vicinity of the defect. Thus, such a reaction is forbidden, no matter what local relaxations take place, because atoms are not free to migrate at temperatures below the glass transition T_g. The charge state of a defect may easily be changed by trapping or emitting carriers, but the chalcogen excess of a defect is permanently fixed. Therefore, Fermi-level pinning reactions must be accomplished by horizontal transitions in Table I. This "selection rule" greatly restricts the number of allowed defect interconversion processes in heteropolar glasses.[22]

It may come as a surprise that the P_2 and P_1 defects are assigned *positive* natural charge states. This is a consequence of the fact that a nonbonding As p orbital is more correctly identified as a conduction-band state than a valence-band state, as will be discussed in Sec. III. If one then considers transitions between the relatively favorable defects in the upper left-hand region of Fig. 2, one finds very few simple candidates for the pinning mechanism. These are shown by arrows in Table I. The most prominent candidates are almost certainly $C_1^- \rightharpoonup (C_3')^+$ and perhaps $C_1^- \rightharpoonup P_4^+$. The others involve bond switching, not simply bond breaking and forming; they require a compensating population of some other negatively charged defects to maintain charge neutrality, and they involve the relatively unfavorable P_2 and P_1 defects (see Sec. IV).

Above T_g, atoms become free to migrate, and an equilibrium is set up among the populations of defects of differing chalcogen excess. The establishment of this equilibrium, which determines the defect densities frozen in at T_g, will be discussed in Sec. IV. We turn now to a discussion of the electronic states associated with the defects of interest.

III. ELECTRONIC STATES

As a starting point, we consider crystalline As_2Se_3. Because the short-range order, or local chemical configuration, is expected to be the most important factor in determining the density of states, we expect the perfect glass to have bands and gaps similar to those in the crystal. As_2Se_3 forms into a layered orpiment structure with 20 atoms per unit cell. Figure 3 shows the theoretical density of states for this structure, as calculated by Bullett[20] using chemical pseudopotentials. It is in good agreement with x-ray photoelectron spectroscopy (XPS) measurements.[24] The Se nonbonding states near −1 eV overlap the σ-bonding-like states near −4 eV to form the principle valence band, and the σ^*-like conduction band is centered near 2 eV. There are also two lower-lying s bands.

In order to make a simplified model, we consider a first-neighbor tight-binding Hamiltonian with just three p orbitals per site. Moreover, each layer is distorted slightly to make all bond angles precisely 90°, so that the structure of Fig. 4(a) results. Since all bonds are now parallel to the x, y, or z axis, the systems of p_x, p_y, and p_z orbitals decouple into three noninteracting subsystems which may be solved independently. The interaction diagram for any one such subsystem, in terms of σ and π bonds, is shown in Fig. 4(b). Next, the bulk perfect glass will be represented by a Bethe-lattice version of this interaction diagram, which is shown in Fig. 5(a). Finally, we will use the cluster-Bethe-lattice method (CBLM)[25] to model defects. For example, a P_2 defect results from breaking a bond in Fig. 4(a); the corresponding CBLM interaction diagrams are shown in Fig. 5(b). Similarly, the interaction diagram for overcoordinated defects or like-atom bonds can be

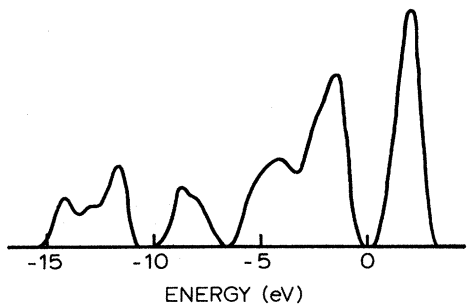

FIG. 3. Theoretical density of states for crystalline As_2Se_3 as given by Ref. 20. The zero of energy is the valence-band maximum.

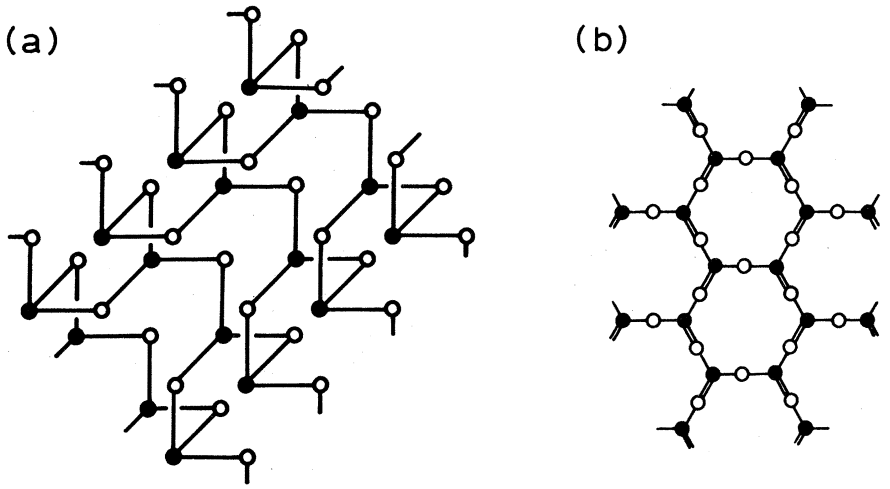

FIG. 4. (a) Right-angle version of As_2Se_3 layer. Solid circles are As, open circles Se. (b) Corresponding interaction diagram for p_x orbitals; double lines represent V_σ, single lines V_π.

modeled as shown in Figs. 5(c) and 5(d).

The resulting model is an elementary example of the CBLM, and is easily solved using Green's-function techniques. Before proceeding, however, it is necessary to comment upon the many simplifying assumptions which went into this model. We have effectively omitted interlayer interactions by choosing a nearest-neighbor Hamiltonian; we have chosen 90° bond angles and omitted s and d orbitals; and we have obscured the ring topology by introducing the Bethe lattice. We have been motivated in these choices by the fact that the interlayer interactions are weak;[26] that the s-p hybridization does not dominate the bonding (average As and Se bond angles are 100 and 94°, respectively, in the crystal)[27]; and that the rings in As_2Se_3 are large and are presumably randomized in the glass anyway. Moreover, we are guided by the philosophy that we are looking for trends when defects are introduced into the glass; it is expected that perturbations due to s states or interlayer interactions will act equally, to a first approximation, upon the defect and bulk states.

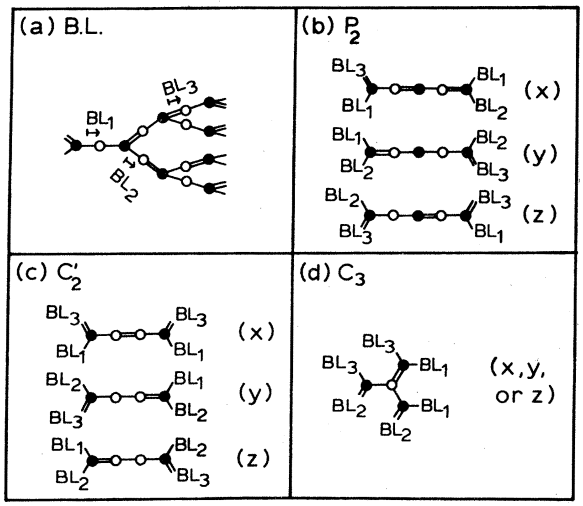

FIG. 5. (a) Interaction diagram for Bethe-lattice structure. Solid circles As, open circles Se; double lines V_σ, single lines V_π. The semi-infinite trees BL_1, BL_2, and BL_3 are defined by the arrows. (b) Interaction diagram for the P_x, P_y, and P_z orbitals of the P_2 cluster-Bethe-lattice structure. Notations at As bonds indicate which semi-infinite tree is to be attached. (c) Same for C_2'. (d) Same for C_3.

A more serious problem is the fact that the calculations are not self-consistent. For this reason, the location of gap states in this model cannot be taken at face value. We will rely here upon the lessons of an earlier study on glassy Se, in which we carried out much more thorough calculations.[16] In addition to a simple tight-binding model for Se, exactly analogous to the one just described for As_2Se_3, we also carried out more sophisticated tight-binding calculations on isolated defects and realistic self-consistent pseudopotential calculations on superlattice structures containing defects. It was found, for example, that self-consistency requires certain tight-binding parameters to be altered in the vicinity of defects. We will frequently argue by analogy to Se in order to predict, in general terms, the effects which would be introduced into our very simple model by self-consistency or other complications.

Let us turn now to a detailed consideration of our elementary model. It contains two kinds of basis orbitals: Se p orbitals, to which we assign energy level $E(p_{Se}) = 0$ by convention, and As p levels at $E(p_{As}) \equiv \Delta$. Since As is more electro-

positive than Se, Δ is positive, and we choose $\Delta = 1.98$ eV following Bullett.[20] These basis levels are shown in the center of Fig. 6. Consider now the bulk Bethe-lattice of Fig. 5(a); focusing on the dominant σ bonding, we note that it contains three kinds of bond orbitals. These are the heteropolar σ and σ^* bond-orbitals and the nonbonding Se p orbital, shown at left in Fig. 6. Taking $V_\sigma = 2.42$ eV (Ref. 28) we find, expressed in units of eV,

$$E(\sigma^*) = \frac{\Delta}{2} + \left[\left(\frac{\Delta}{2}\right)^2 + V_\sigma^2\right]^{1/2} = 3.54, \tag{2a}$$

$$E(p_{Se}) = 0, \tag{2b}$$

$$E(\sigma) = \frac{\Delta}{2} - \left[\left(\frac{\Delta}{2}\right)^2 + V_\sigma^2\right]^{1/2} = -1.65. \tag{2c}$$

When π interactions are included [we let $V_\pi = 1.05$ eV (Ref. 28)] and the Bethe-lattice model is solved using standard Green's-function techniques,[25] the σ and σ^* levels broaden into the bands shown at the extreme left of Fig. 6. The lone-pair band occurs at $E = 0$ eV but remains unbroadened, a peculiar artifact of the bonding geometry of the model. It therefore avoids overlapping with the σ-bonding band, leaving a secondary gap where the real glass has none. The σ and lone-pair bands are valence bands, while the σ^* band forms the conduction band. In our model, the fundamental gap occurs between 0 eV and

$$E(\sigma^* \text{ band min}) = \frac{\Delta}{2} + \left[\left(\frac{\Delta}{2}\right)^2 + (V_\sigma + V_\pi)^2\right]^{1/2} \tag{2d}$$

or 2.61 eV.

Also shown at the right of Fig. 6 are the other five simple bond orbitals which can occur in glassy As_2Se_3, but only in the presence of defects. Note that several of these bond orbitals (the nonbonding p_{As} orbital and the homopolar σ^*_{Se} and σ_{As} orbitals) have energy levels within, or close to, the fundamental gap:

$$E(\sigma^*_{Se}) = V_\sigma = 2.42, \tag{2e}$$

$$E(p_{As}) = \Delta = 1.89, \tag{2f}$$

$$E(\sigma_{As}) = \Delta - V_\sigma = -0.53, \tag{2g}$$

all expressed in eV. As we shall see, it is these orbitals which give rise to the gap states of interest in As_2Se_3. It is the electronegativity difference which is responsible for raising the p_{As} level out of the lone-pair band, and shifting the σ_{As} and σ^*_{Se} levels out of the σ and σ^* bands.

Let us begin our survey of defects by considering the simple like-atom bonds. This is a class of defects which has no counterpart in glassy Se. In Figs. 7(a) and 7(b) we present the density of states (as obtained from the Green's function) for the bulk Bethe lattice and for the C_2' defect (Se LAB), respectively. The locations of the σ, p_{Se}, and σ^*

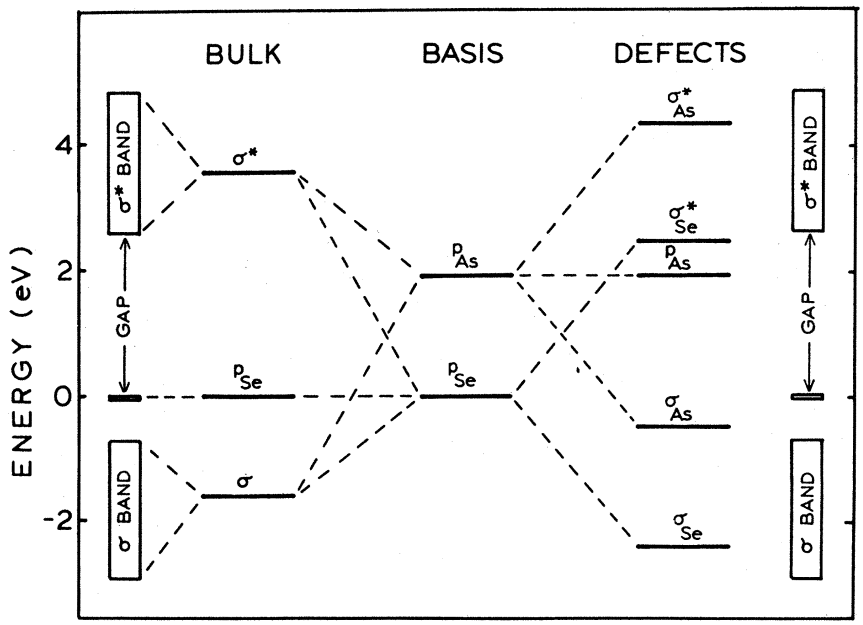

FIG. 6. Energy levels relevant to a-As_2Se_3, as determined from simple model of text. σ interactions between basis p orbitals (center) give rise to bulk bond orbitals (left) and defect bond orbitals (right). π interactions between the former in turn give rise to Bethe-lattice bulk bands (extreme left, repeated extreme right for reference).

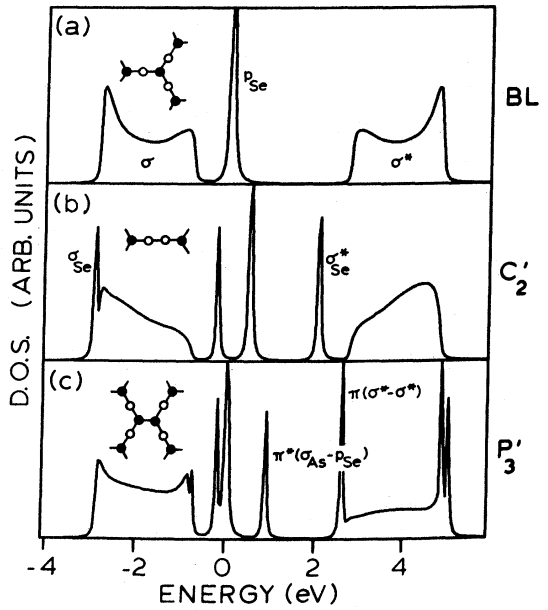

FIG. 7. (a) Density of states for Bethe-lattice structure. (b) Local density of states, averaged over sites near the defect, for C_2' like-atom bond. (c) Same for P_3' like-atom bond. Certain features discussed in the text are labeled according to their dominant character. Schematic diagrams show the structure (solid circles As, open circles Se; external As bonds are understood to have Bethe-lattices attached). The fundamental gap extends from 0 to 2.61 eV. Note that a Lorentzian broadening of half-width 0.05 eV has been introduced by the Green's-function calculation.

bulk bands in Fig. 7(a) correspond exactly with those shown at the extreme left of Fig. 6. The new features which arise at the C_2' defect can be understood by referring to the corresponding interaction diagrams in Fig. 5(c). Note that the system of x orbitals contains a new σ-bonded pair of p_{Se} orbitals. The resulting σ^*_{Se} level falls within the gap at 2.42 eV (see Fig. 6); when embedded in the bulk, it is shifted slightly deeper into the gap by the π interactions to form the state at 2.02 eV, below the conduction-band edge in Fig. 7(b). (The defect is neutral when this state is unoccupied.) Similarly, there is a σ_{Se} state appearing just at the bottom of the bonding band. (There is also some splitting of states out of the lone-pair band due to slight changes in the interactions near the defect, but this may be an artifact of the lack of lone-pair bandwidth.) We expect the situation to be similar for the states of the C_2'' defect, which appears in the raft model of Phillips.[7]

The situation for the P_3' defect of Fig. 7(c) is similar, but now a pair of As p orbitals give rise to σ_{As} and σ^*_{As} bond orbitals. Notice from Fig. 6 that the σ_{As} level lies quite close in energy to the Se nonbonding orbitals. In fact the σ_{As} bond orbital interacts via a direct π interaction with two neighboring p_{Se} orbitals, giving rise to π and π^* complexes. The π^* complex would occur at

$$E_\pi^*(\sigma_{As}-p_{Se})=\frac{E(\sigma_{As})}{2}+\left[\left(\frac{E(\sigma_{As})}{2}\right)^2+V_\pi^2\right]^{1/2} \tag{2h}$$

or 0.82 eV, if isolated. This is the origin of the gap state at 0.87 eV in Fig. 7(c). (The defect is neutral when this gap state is fully occupied.) Presumably this state will not be quite so far above the valence-band edge when a lone-pair band of nonzero width is considered, and it may be inhomogenously broadened by variations in the local environments of the defects. Finally, notice that a state appears to emerge just at or below the conduction-band edge as well. This occurs because the σ^* bandwidth results from π interactions which couple the Se side of one σ^* bond orbital to the As side of the next, while the π interaction along the As–As bond couples to the As side of both σ^* orbitals. The σ^* orbitals have more As than Se character (a consequence of the electronegativity difference), so the effective interaction at the As–As bond is atypically large, resulting in π and $\pi^*(\sigma^*-\sigma^*)$ levels just below and above the conduction-band edges.

Next, we turn to the simple coordination defects. Figures 8(a) and 8(b) show the density of states in the vicinity of an under- or overcoordinated Se atom, respectively. One finds no deep gap states, although the additional interactions among σ and σ^* orbitals in the neighborhood of the C_3 defect give rise to strong resonances near the corresponding band edges. The lack of deep gap states is a consequence of the fact that no novel bond orbital or interaction has been introduced. This is unlike the case of C_1 and C_3 defects in amorphous Se, where a direct π interaction between nonbonding or σ^* orbitals gives rise to deep gap states. In As_2Se_3, direct π interactions between σ^* orbitals already occur in the bulk, and no direct π interactions between Se nonbonding orbitals (NBO's) are introduced by the C_1 defect, because the neighboring site contains an As atom.

At this point we must point out that the single MCA defects are not neutral in their natural charge states, unlike the LAB's. The C_1 and C_3, for example, have charges −1 and +1, respectively, if the valence bands are fully occupied and the conduction band empty. This means that while these defects will *not* support deep gap states, they *will* support hydrogenic acceptor and donor levels. Consider, for example, the neutral C_3 defect, which has one electron in the conduction band. If that electron were localized to the defect site, each atom would be approximately neutral,

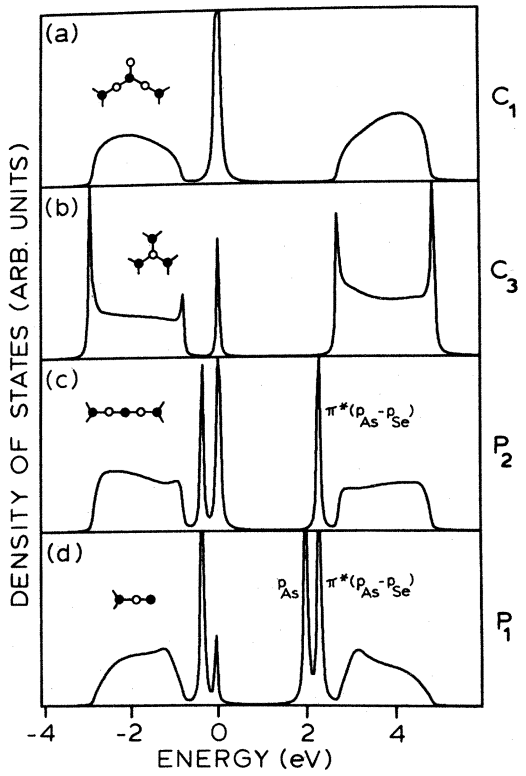

FIG. 8. Local density of states for simple malcoordinated atom defects. (a) C_1, (b) C_3, (c) P_2, and (d) P_1. Details of Fig. 6 apply.

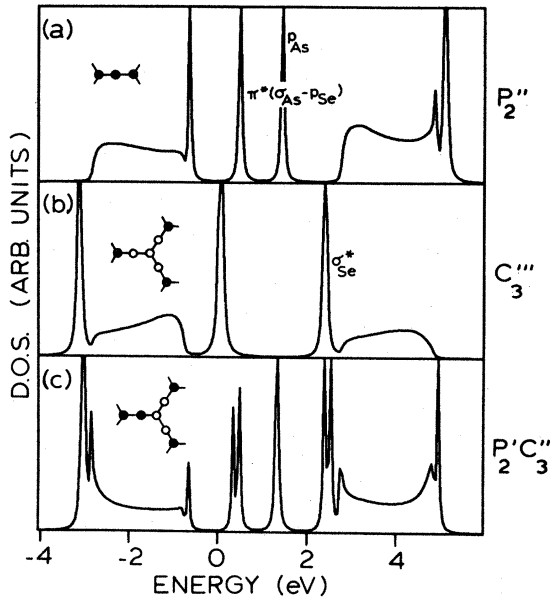

FIG. 9. Local density of states for substitution and exchange defects. (a) P_2'', (b) C_3'', and (c) $P_2'C_3''$. Details of Fig. 6 apply.

and self-consistency would not be important. Instead, that electron tries to go into a conduction-band state, leaving behind a positive charge which in fact traps the electron in a hydrogenic orbit. The same self-consistency argument applies to a hole on the neutral C_1 defect, which gives rise to a hydrogenic acceptor level.

Unlike the C_1 and C_3, the undercoordinated P_2 and P_1 defects *do* introduce a new bond orbital, namely, an As nonbonding orbital. When isolated, this orbital lies at $E=\Delta$, below the conduction-band edge. In the P_2 defect it interacts with a Se NBO via a direct π interaction, and moves further upward ~0.3 eV, to form the state at 2.27 eV in Fig. 8(c). In the P_1 there is a second NBO which remains near its unperturbed energy on the same As site, giving rise to a second defect state in Fig. 8(d).

For a neutral P_2 the gap level is half-occupied, and for a P_1 the lower gap level is fully occupied while the higher one is empty. Self-consistency should not be important at these defects, because the gap states are well localized and the sites comprising the defect are therefore individually neutral. Note that if the Fermi level falls near midgap (as it is known to do experimentally), the P_2 and P_1 will carry charge +1 and +2, respectively. The usual picture of coordination defects in chalcogenides considers the undercoordinated defects to be naturally negatively charged, but the conventional wisdom fails here because the As NBO level falls closer to the conduction band than to the valence band. This unusual state of affairs is due to the electronegativity difference, which shifts the p_{As} level well above the p_{Se} valence levels (see Fig. 6). Physically, a P_2^- is unfavorable because the extra electron would be highly localized to an electropositive As site. Of course, in a lone-pair semiconductor, the unoccupied As p orbitals on the P_2^+ will be unstable towards dative bonding with a neighboring p_{Se} (or even s_{As}) lone pair.[21] Thus it appears that undercoordinated pnictide defects are unlikely to occur at all (see also Sec. IV). However, if local bonding constraints occasionally forbid such dative bonding, we expect the resulting defects to be positively charged.

The last class of defects to be considered explicitly will be the substitutions and interchanges. As pointed out in Sec. II, these are likely to occur as defects in crystalline As_2Se_3, or perhaps as a consequence of the LCAB principle in the glass. If an As atom is substituted for a Se, the P_2'' defect of Fig. 9(a) results. The LAB's give rise to the twofold degenerate σ_{As} level near 0.45 eV, and the As NBO on the P_2 site gives rise to the level near midgap. (It lies lower in energy than in the P_2 because of an interaction with σ^* orbitals.) The defect is neutral when the As NBO is half-occupied; this state is highly localized and self-consistency

should not be important. The resulting picture is quite consistent with the work of Bullett,[20] who has carried out chemical pseudopotential calculations on the substitutional defects. (In the latter calculation, the introduction of the correct bond angles breaks the twofold degeneracy, giving rise to a pair of σ_{As}-like states above the valence-band edge.)

Figure 9(b) shows the density of states near the C_3''' defect, in which a Se atom has replaced an As. The gap state below the conduction-band edge is threefold degenerate and has most of its character on σ^*_{Se} orbitals at the defect. Just as for the C_3 defect in pure Se, the threefold degeneracy will be broken when the bond angles are allowed to differ from 90°, and a nondegenerate state will fall somewhat lower in the gap. Self-consistency arguments suggest that this state will be lowered further still by the negative self-energy shift at the defect site which is necessary to restore charge neutrality. Once again we have good agreement with the previous results of Bullett,[20] who finds a triplet of gap states centered ~0.4 eV below the conduction-band edge.

Finally, the result of interchanging nearest-neighbor As and Se atoms is shown in Fig. 9(c). The density of states resembles a superposition of the C_3''' and P_2'', except that the degenerate orbitals have been split by the lowered symmetry. The defect is neutral when the As NBO state near midgap contains two electrons. It would be quite possible to go on considering more complicated defects in detail. As the last examples illustrate, however, once we have understood the nature of the gap states introduced by individual LAB's and MCA's, the essential features of the more complex composite defects can readily be predicted.

IV. DEFECT CREATION ENERGIES

We shall end this paper with some brief speculations about defect creation energies, defined as the ground-state total energy of a given defect configuration minus that of the same set of atoms in the bulk. The electronic contribution to this difference is[19]

$$\delta E_{el} = \sum_i \int_{-\infty}^{\epsilon_f} \epsilon[\eta_i(\epsilon) - \eta_i^0(\epsilon)]d\epsilon , \tag{3}$$

where η_i and η_i^0 are the local density of states on atom i for the defect and bulk configurations, respectively. This is not the entire expression for the total energy, however, because the latter also includes the Coulomb repulsion between cores and other corrections. If these are modeled as a constant repulsive energy R per bond,[16,29,30] the resulting contribution is

$$\delta E_R = \frac{R}{2} \sum_i (c_i - c_i^0) , \tag{4}$$

where c_i and c_i^0 correspond to the coordination number of the ith site in the defect and bulk, respectively. Finally, the defect creation energy is

$$E_{tot} = \delta E_{el} + \delta E_R + Q_e \mu_e - Q_c \mu_c . \tag{5}$$

Here Q_e is the charge on the defect and Q_c is the chalcogen excess. The chemical potentials μ_e (Fermi level) and μ_c are introduced as a reminder that the difference in energies of two defects with different charge states, or different chalcogen excess, is not uniquely defined. However, the heat of reaction for any physically realizable defect interconversion process is independent of the chemical potentials, since numbers of electrons and atoms must be conserved.

Estimates of defect total energies are notoriously difficult; realistic calculations are available only for pure Se,[17] and these demonstrate that simple models which are based solely upon discreet bond-orbital energies, and which neglect intercore repulsion, give decidedly inadequate results. Adler[30] has recently modified such a simple model to include a constant repulsive R per bond, in order to give zeroth-order defect energy estimates. However, such a model still does not include the effects of nonzero bandwidths or gap states and resonances; nor can it account for electronegativity differences, charge transfers, or the partial ionic character of bonds in the heteropolar glasses.

As was pointed out in Sec. II, the latter effects are expected to give the simple LAB defects a creation energy on the order of 0.2 eV. The creation energy of MCA's, however, is undoubtedly larger ($\gtrsim$0.5 eV in Se)[31] and much harder to estimate. The electronic binding energy gained (lost) in forming (breaking) a bond will be at least partly compensated by the corresponding δE_R. It may be overcompensated, in which case the bond will prefer not to form; it is difficult to predict, *a priori*, whether this will be so. In the case of pure Se, it was found that the bond prefers to be broken, i.e., $C_3^0 \rightarrow C_1^0$ is exothermic.[17] However, this is largely due to the anomalous π interaction which stabilizes the C_1 defect; we have shown this does *not* occur at the C_1 defect in As_2Se_3. In fact, none of the simple MCA's (C_1, C_3, P_2, P_1) shows analogous π-bond stabilization, and it is likely that the corresponding creation energies are closer than in pure Se. The $(C_1')^0$ defect will, on the other hand, exhibit this π-bond stabilization, and it may be lower in energy than the C_1^0 despite the necessity of adding a LAB.

There is some reason to expect the chalcogen

MCA's to be preferred over the pnictide ones. Adler[30] points out that the Coulomb U for creating the P_2^- (or P_2^+) involves placing two electrons (or holes) on a highly localized orbital, and is therefore larger than for the C_1 or C_3. Moreover, the neutral C_1 or C_3 has a hole or electron in a band-edge state, rather than at the bond-orbital energy (band center); this lowers the energy with respect to the zeroth-order model. The corresponding stabilization does not take place for P_2 or P_1 defects, again because of the deep gap nature of the As NBO levels.

It has been proposed[21] that the electronegativity difference will favor the P_4^+ defect over the C_3^+, and the C_1^- over the P_2^-. However, this will only be the case if the extra electron or hole is constrained to reside on the defect site itself. As shown in Sec. III, the P_2^- is quite unfavorable for this reason, with the extra electron localized predominantly to a single As NBO. On the other hand, the argument fails for the C_3^+, in which the added hole is shared by σ^* orbitals which have more As than Se character. (For the same reason, the C_3^0 cannot be ruled out as the source of the broad "As center" seen in optically induced ESR experiments.[31]) In the absence of compelling arguments to the contrary, we therefore follow Adler[30] in assuming that the large s-p promotion energy makes P_4 defects relatively unfavorable, although this may be compensated in part by the increased strength of the more highly directed tetrahedral bonds.

Of course, defects must occur in pairs (or triplets, etc.) whose total charge and chalcogen excess are constrained to zero in pure As_2Se_3. If we assume that the defects are frozen in at the glass transition temperature T_g,[5] then the density of each defect is $n_0 \exp(-E_{tot}/kT_g)$, with n_0 being roughly the density of atomic sites and E_{tot} given by Eq. (5). The chemical potentials μ_e and μ_c are then determined by the requirements of charge neutrality and the stoichiometric ratio of the glass. For example, the estimate of Eq. (1) suggests that the neutral C_2' and P_3' LAB's will be by far the most common defects. In order to have an As_2Se_3 alloy we require the densities of the two defects to be equal

$$n_0 e^{-E_{tot}(C_2')/kT_g} \cong n_0 e^{-E_{tot}(P_3')/kT_g}. \tag{6}$$

Since $\delta E_R = Q_e = 0$, $Q_c = \pm 1$ for these defects, Eq. (5) gives

$$\mu_c \cong \tfrac{1}{2}[\delta E_{el}(C_2') - \delta E_{el}(P_3')] \tag{7}$$

and

$$n(C_2') \cong n(P_3') \cong n_0 \exp\{-\tfrac{1}{2}[\delta E_{el}(C_2') + \delta E_{el}(P_3')]/kT_g\}. \tag{8}$$

(Note that if the defects occur only in close pairs,[9] the Boltzmann prefactor would be the *sum* rather than the *average* of the C_2' and P_3' energies, and a considerably lower density of defects would occur, reflecting the loss of the entropy of mixing.[21] Therefore distant pairs will predominate unless the binding energy of a pair exceeds the average creation energy, which is unlikely for neutral defects.)

μ_c is plausibly on the order of a tenth of an eV or less, so that the last term of Eq. (5) is probably never very important for coordination defects. That is, the chalcogen excess of the coordination defects in As_2Se_3 (which presumably pin ϵ_f) is not constrained to balance, since it can easily be compensated by LAB's elsewhere in the glass. For the same reason, the concentrations of the various coordination defects are not expected to be highly stoichiometry dependent.

The picture which emerges of the glass at T_g, then, is of a fairly high density (perhaps $\sim 10^{20}$ cm^{-3}) of LAB defects. If the P_3' gives rise to a σ_{As}-like states above the valence-band edge as expected, the observed intrinsic hole mobility must be governed by extended state conduction or fast hopping among this manifold of states, as suggested by Halpern.[9] Scattered among the LAB's would be a smaller number ($\sim 10^{18}$ cm^{-3}) of charged coordination defects. These would be dominated by the lowest-energy charge-compensated pair [possibly C_1^- and C_3^+, which would occur, for example, at a density of

$$n_0 \exp\{-\tfrac{1}{2}[\delta E_{el}(C_1^-) + \delta E_{el}(C_3^+)]/kT_g\} \tag{9}$$

in analogy to Eq. (8)]. One or both members of this pair could then give rise to the neutral excitations responsible for the photoinduced phenomena, and to the negative-U pinning of the Fermi level via one of the horizontal reactions in Table I, e.g., $C_1^- \rightleftharpoons (C_3')^+$.

This picture is admittedly speculative, and the identification of those defects actually involved would require realistic total energy calculations or new experimental information. Moreover, the effects of interactions between charged defects may be important, and have not been discussed above. Nevertheless, given our present state of knowledge in this area, we believe this description to be a plausible starting point for developing a viable model for defects in the heteropolar chalcogenides.

V. SUMMARY AND CONCLUSIONS

We have developed a scheme for classifying and labeling defects in terms of the constituent like-atom bonds (LAB's) and malcoordinated atoms (MCA's). The concept of like-coordinated-atom

bonds (LCAB's) is also discussed, and the fact that LCAB's are suppressed for defects in crystalline As_2Se_3 is offered as a possible explanation for experimental indications that certain nonradiative recombination centers occur only in the glass. We have shown that each defect is characterized by a chalcogen excess which characterizes its contribution to the deviation from an exact 2:3 stoichiometry, and we have pointed out that conservation of chalcogen excess imposes a constraint upon the possible defect interconversion processes which can pin the Fermi level below T_g.

Next, an elementary Bethe-lattice model is presented and solved for a selection of simple defects involving LAB's and MCA's. While the results of such a simple model cannot be taken at face value, we know how they are modified in more realistic (e.g., self-consistent) calculations for Se, and we can use this knowledge to predict the gross features of a realistic calculation in As_2Se_3. Our primary result is that defects in As_2Se_3 are quite different from those in Se, and arise for entirely different reasons. While in Se, gap states arise at onefold and threefold sites because of unique π bonding between bond orbitals on the defect and its neighbors, in As_2Se_3 they are associated with unique bond orbitals (like-atom bond σ and σ^* orbitals and As NBO's). Thus, while C_1 and C_3 defects give rise to deep gap states in Se, they admit only hydrogenic levels in As_2Se_3. Deep states do exist, however, at LAB's and at undercoordinated pnictide sites. We believe that the latter defects (P_2 and P_1) will *not* be negatively charged, as previously thought, but rather *positively* charged due to the position of the As nonbonding p orbitals near the conduction-band edge in As_2Se_3.

Finally, we discuss the structural equilibrium of the glass at T_g, and introduce a new chemical potential μ_c which reflects the relative abundance of chalcogen atoms with respect to pnictides. We argue that the creation energies of the simple LAB's will be low (and will fix μ_c), so that a large number of LAB's (perhaps $\sim 10^{20}$ cm^{-3}) will permeate the glass. We then suggest that a smaller density (perhaps $\sim 10^{18}$ cm^{-3}) of coordination defects, predominantly on chalcogen sites, is responsible for the negative-U properties and the pinning of the Fermi level.

ACKNOWLEDGMENTS

This work was supported in part by NSF Grant No. DMR 76-80895. The authors wish to thank Marc Kastner, Gregg Higashi, and Joseph Orenstein for helpful discussions.

[1] P. W. Anderson, Phys. Rev. Lett. 34, 953 (1975).
[2] P. W. Anderson, J. Phys. (Paris) 10, Suppl. C4-339 (1976).
[3] D. C. Licciardello, D. L. Stein, and F. D. M. Haldane, Philos. Mag. (in press).
[4] N. F. Mott, E. A. Davis, and R. A. Street, Philos. Mag. 32, 961 (1975).
[5] M. Kastner, D. Adler, and H. Fritzsche, Phys. Rev. Lett. 37, 1504 (1976).
[6] M. Kastner, J. Non-Cryst. Solids 35-36, 807 (1980).
[7] J. C. Phillips, A. C. Beevers, and S. E. B. Gould, Phys. Rev. B 21, 5724 (1980).
[8] E. N. Economou, K. L. Ngai and T. L. Reinecke, *Linear and Non-Linear Electron Transport in Solids* (Plenum, New York, 1976), p. 595.
[9] V. Halpern, Philos. Mag. 34, 331 (1976).
[10] K. L. Ngai and P. C. Taylor, Philos. Mag. B 37, 175 (1978).
[11] D. Emin, J. Non-Cryst. Solids 35-36, 969 (1980), and references therein.
[12] G. S. Higashi and M. Kastner, J. Phys. C 12, L821 (1979).
[13] J. Orenstein, and M. Kastner (unpublished).
[14] M. Abkowitz and R. C. Enck, J. Non-Cryst. Solids 35-36, 831 (1980).
[15] M. Abkowitz, Bull. Am. Phys. Soc. 25, 231 (1980).
[16] D. Vanderbilt and J. D. Joannopoulos, Phys. Rev. Lett. 42, 1012 (1979).
[17] D. Vanderbilt and J. D. Joannopoulos, Solid State Commun. 35, 535 (1980).
[18] S. G. Bishop, U. Strom, and P. C. Taylor, J. Non-Cryst. Solids 32, 359 (1979).
[19] D. Vanderbilt and J. D. Joannopoulos, Phys. Rev. B 22, 2927 (1980).
[20] D. W. Bullett, Phys. Rev. B 14, 1683 (1976).
[21] M. Kastner and H. Fritzsche, Philos. Mag. B 37, 199 (1978).
[22] R. A. Street and G. Lucovsky, Solid State Commun. 31, 289 (1979).
[23] R. A. Street, Adv. Phys. 25, 397 (1976).
[24] S. G. Bishop and N. J. Shevchik, Phys. Rev. B 12, 1567 (1975).
[25] J. D. Joannopoulos and F. Yndurain, Phys. Rev. B 10, 5164 (1974).
[26] R. Zallen and M. Slade, Phys. Rev. B 9, 1627 (1974).
[27] A. C. Larson and D. T. Cromer, Acta Cryst. B 29, 1583 (1973).
[28] W. B. Pollard and J. D. Joannopoulos, Phys. Rev. B 19, 4217 (1979).
[29] D. J. Chadi, Phys. Rev. Lett. 41, 1062 (1978).
[30] D. Adler, J. Non-Cryst Solids 35-36, 819 (1980).
[31] S. G. Bishop, U. Strom, and P. C. Taylor, Phys. Rev. B 15, 2278 (1977).